Injection of glycosylated recombinant simian IL-7 provokes rapid and massive T-cell homing in rhesus macaques

Stéphanie Beq,[1] *Sandra Rozlan,[2] *David Gautier,[1] Raphaëlle Parker,[1] Véronique Mersseman,[1] Clémentine Schilte,[1] Brigitte Assouline,[2] Iann Rancé,[2] Pascal Lavedan,[3] Michel Morre,[2] and Rémi Cheynier[1]

[1]Département de Virologie, Institut Pasteur, Paris; [2]Cytheris SA, Technopolis, Issy les Moulineaux; and [3]Animalerie Centrale, Institut Pasteur, Paris, France

Interleukin-7 (IL-7), the principal cytokine implicated in thymopoiesis and peripheral T-cell homeostasis, is presently under evaluation in human diseases characterized by persistent lymphopenia. Unexpectedly, before the eventual IL-7–driven T-cell expansion, all treated patients showed a profound T-cell depletion 24 hours after injection. The current study uses the rhesus macaque model to investigate the mechanisms involved in this IL-7–induced T-cell depletion. We identify a new critical function of IL-7 that induces massive and rapid T-cell migration from the blood into various organs, including lymph nodes, parts of the intestine, and the skin. This homing process was initiated after the induction of chemokine receptor expression by circulating T cells and the production of corresponding chemokines in target organs. Finally, we demonstrate that the IL-7–induced cell cycling is initiated within these organs before T cells migrate back into the bloodstream, indicating that T-cell homing is required for in vivo IL-7 function. (Blood. 2009;114:816-825)

Introduction

Interleukin 7 (IL-7), the cytokine that promotes precursor B- and T-cell maturation[1-3] and sustains peripheral T-cell homeostasis,[4-6] is currently in phase 1/2 trials in diseases characterized by persistent lymphopenia. Although interim results from these investigations tentatively support the efficacy of this molecule in producing long-term T-cell increases in patients, an unexpectedly strong T-cell depletion was observed in all treated patients during day 1 of therapy[7] (Irini Sereti, National Institute of Allergy and Infectious Diseases, personal oral communication, June 2008). Similar transient T-cell depletion was previously observed in both $CD4^+$ and $CD8^+$ T-cell subsets in IL-2–treated HIV-1–infected patients. In this study, massive apoptosis was observed at the end of the IL-2 cycle coinciding with the peak of proliferation.[8] Although apoptosis is not observed under physiologic concentrations of IL-7 in culture, during the first hours after IL-7 injection in patients the pharmacologic IL-7 plasma concentration may result in a different outcome. Otherwise, T-cell depletion may also be the consequence of a massive T-cell redistribution.

Various chemokine-chemokine receptor couples participate in specific T-cell homing into both lymphoid and nonlymphoid organs.[9] In particular, CCL19-CCR7, CCL21-CCR7, and CXCL12-CXCR4 are primarily implicated in recruiting T cells into secondary lymphoid organs,[10,11] whereas CCL20-CCR6 interaction drives T cells to the gut[12] and CCL25 allows CCR9-expressing T cells to home to the small bowel.[12,13] Engagement of the chemokines with their receptors on the leukocyte membranes triggers intracellular signals resulting in tight adhesion of the migrating cells through integrins, extravasation from the bloodstream into tissues along chemokine gradients, eventually allowing cell activation. Interestingly, in vitro IL-7 stimulation was shown to induce CXCR4 expression by naive T cells, suggesting potential homing consequences.[14]

IL-7 is constitutively produced by stromal and epithelial cells in the bone marrow,[15] thymus,[16] and lymph nodes[6,17-19] but also in the skin[20] and mucosal tissues.[21] Its affinity for heparan sulfate proteoglycans (HSPGs) on the stromal cells[22,23] suggests that a higher local IL-7 concentration in productive tissues than in plasma may play a role in its functions. Contrary to the situation in the thymus, where IL-7 interaction with HSPG does not seem required,[24] HSPGs provide a docking site for IL-7 in the bone marrow, controlling its availability to B-cell precursors.[23] In the other sites of IL-7 production, the implications of local IL-7 concentration on its function remain to be clarified.

After confirming in the healthy rhesus macaque model that the injection of recombinant glycosylated simian IL-7 (R-sIL-7gly) is, as in human patients, immediately followed by massive depletion of circulating T cells, we investigated the consequences of R-sIL-7gly injection on both T-cell apoptosis and T-cell homing.

Methods

Animal care and treatment

The rhesus macaques included in this study were handled in accordance with European guidelines for care and treatment of research animals, and the experiments performed on them were approved by the ethics committee of the Institut Pasteur. The animals were seronegative for SIVmac, simian T-cell leukemia virus type 1, simian retrovirus type 1 (type D retrovirus), and herpes virus B. For all injections and blood draws, the animals were anesthetized with ketamine (Imalgène 1000; Mérial).

Submitted November 24, 2008; accepted March 26, 2009. Prepublished online as *Blood* First Edition paper, April 7, 2009; DOI 10.1182/blood-2008-11-191288.

*S.R. and D.G. contributed equally to this work.

An Inside *Blood* analysis of this article appears at the front of this issue.

The online version of this article contains a data supplement.

The publication costs of this article were defrayed in part by page charge payment. Therefore, and solely to indicate this fact, this article is hereby marked "advertisement" in accordance with 18 USC section 1734.

In the first phase of the experiment, 2 healthy rhesus macaques of Chinese origin (no. 14424 and no. 14694) and an animal (no. 17021) previously immunized against simian IL-7 received a single subcutaneous injection of recombinant glycosylated simian IL-7 (R-sIL-7gly; 80 μg/kg body weight), a dose previously shown to stimulate T-cell expansion in both healthy and SIV-infected macaques.[25,26] Macaque no. 17021, extensively immunized with 3 injections of nonglycosylated recombinant simian IL-7 and complete Freund adjuvant, demonstrated significant levels of anti–IL-7–neutralizing antibodies (> 1/2500) at the time of the experiment. After R-sIL-7gly injection, blood samples (3 mL on ethylenediaminetetraacetic acid) were drawn from both treated animals at 6, 12, 48, and 96 hours, as well as at day 7 and day 14. In addition, 2 noninjected animals (no. 21045 and no. 26007) served as controls and were subjected to the same sampling protocol. Four months later, when all the measured parameters had returned to baseline levels, macaques no. 14424 and no. 14694 received a second injection of R-sIL-7gly. Macaques no. 26007 and no. 21045 served as controls. Blood samples were drawn at 6, 12, 48, and 96 hours (H0 to H96), as well as at day 7. Moreover, at H0, H6, and H24, axillary or inguinal lymph nodes were surgically removed from macaques no. 14424, no. 14694, and no. 26007 at H0, H6, and H24.

In a second phase of the experiment, 3 healthy rhesus macaques were subcutaneously injected with R-sIL-7gly (80 μg/kg body weight) and killed at day 1 (no. 26007-2 and no. 41127-2) and day 7 (no. 40885-2). A fourth animal (no. 21045-2) without R-sIL-7gly injection was killed as a negative control. For this experiment, we also used historical samples from a healthy macaque, kindly provided by Dr Cécile Butor (Institut Cochin, Département d'Immunologie, Inserm U567, CNRS UMR8104, Université Paris-Descartes, Faculté de Médecine, Paris and Université Paris 7, Denis Diderot, France).

Immunophenotyping and flow cytometric analysis

For fluorescence-activated cell sorter (FACS) analysis performed on total blood samples, ethylenediaminetetraacetic acid-treated blood cells were incubated for 15 minutes with conjugated monoclonal antibodies (mAbs). For intracellular labeling, cells were permeabilized with the Cytofix/Cytoperm Kit (BD Biosciences) before incubation with specific mAbs after the manufacturer's instructions. Erythrocytes were lysed with the Beckman Coulter Lysing Kit according to the manufacturer's instructions. Samples were then washed and fixed in 2% paraformaldehyde phosphate-buffered saline (PBS, PFA 2%). Immunostainings were produced using a Cyan cytofluorometer (Dako) and analyzed with FlowJo 8.7 software (TreeStar).

For FACS analysis of tissue samples, cell suspensions were obtained by scraping and mild enzymatic dissociation in PBS containing 20 U/mL collagenase VII (Sigma-Aldrich) and 40 U/mL DNase I (Sigma-Aldrich) in 2% fetal calf serum for 30 minutes at 37°C.

The different monoclonal antibodies used in this study were: CD3-allophycocyanin-Cy7, CD4-peridinin chlorophyll protein-Cy5.5, CD28-phycoerythrin (PE), CD95-allophycocyanin purchased from BD Biosciences; CD8-PE-Cy7, CD31biotin, streptavidin-PE-Texas-Red and CD31-DY590 (Proteogenix) Ki-67-fluorescein isiothiocyanate (FITC) and Bcl-2-FITC from Dako; CCR7-FITC, CCR6-FITC, CCR9-FITC, and CXCR4-FITC (R&D-Lille); caspase 8 and caspase 9 (Abcam).

Immunohistochemistry

Snap-freezing was performed using Cryomold (Tissue-Tek) and optimal cutting temperature compound (OCT Tissue-Tek). The cups were placed in isopentane and cooled in liquid nitrogen. Samples were then stored at −80°C until used.

Frozen tissue sections were used for immunohistochemical detection of CD3, CD127, and Ki-67 molecules. Briefly, frozen tissue sections with a thickness of 4 μm were prepared and mounted on glass slides. The sections were then air dried for 1 hour and fixed with acetone for 10 minutes. Before immunolabeling, the sections were fixed with acetone/methanol (50/50) for 5 minutes at room temperature and then rehydrated with Tris-buffered saline, pH 7.6 (Dako), for 5 minutes at room temperature. Endogenous peroxidase activity was blocked with hydrogen peroxide 3% for 5 minutes at room temperature. To reduce nonspecific background binding of the secondary antisera, sections were incubated for 20 minutes with rabbit serum. Sections were then incubated for 1 hour with primary antibody and subsequently incubated with biotinylated rabbit anti–mouse immunoglobulin (Dako) for 30 minutes, followed by streptavidin biotin peroxidase complex for an additional 30 minutes. Each incubation was followed by a PBS wash. To facilitate visualization of the reaction, diaminobenzidine was added to the sections, which were then counterstained with Mayer hematoxylin and mounted under Shandon synthetic montant (Thermo Electron). Slides were examined using an Eclipse E800 microscope and a DXM1200 digital camera (Nikon). Images were acquired using ACT-1 software (Nikon).

Table 1. Oligonucleotides used for chemokine mRNA quantification

Name	Sequence
CCL19-Out5	ACCGTTGGCCTGCCTCTGTT
CCL19-In5	CAGCCTGCTGGTTCTCTGGA
CCL19-Out3	CTGCTGCGGCGCTTCATCTT
CCL19-In3	TCCTCTGCAGTCTCTGGAT
CCL20-out5	CCATGTGCTGTACCAAGAGT
CCL20-In5	TTGCTCCTGGCTGCTTTGA
CCL20-out3	TGCTGAGGCGACGTACAATA
CCL20-In3	CCCAGGTCTGCTTTGGATT
CCL21-out5	CCTCAGCTCTGGCCTCTTA
CCL21-In5	ATGGCTCAGTCACTGGCTCT
CCL21-out3	TCACTGGGCTATGGCCCTTTA
CCL21-In3	CTATGGCCCTTTAGGGGTCT
CCL25-out5	CACACCCAAGGTGTCTTTGA
CCL25-In5	TTATCGGATCCAGGAGGTGA
CCL25-out3	TTAGCTGATGTCAGGAGGGA
CCL25-In3	CTGCTGGTGGGATTGCTAAA
HPRT-Out5	CTGAACGTCTTGCTCGAGAT
HPRT-Out3	CGACCTTGACCATCTTTGGA
HPRT-In5	CACATTGTAGCCCTCTGTGT
HPRT-In3	CTGACCAAGGAAAGCAAAGT

Chemokine quantification

Primers specific for each chemokine (CCL19, CCL20, CCL21, CCL25) and the HPRT gene (used as a housekeeping gene) were based on macaque cDNA sequences (accession nos. ENSG00000172724, ENSG00000115009, ENSG00000137077, ENSG00000131142, and ENSG00000165704). The oligonucleotides used for chemokine quantifications are shown in Table 1. Polymerase chain reaction (PCR) products obtained with the outer primer pairs for each chemokine were cloned, together with the out hypoxanthine phosphoribosyl transferase (HPRT) amplicon, into a Topo cloning vector (Invitrogen) and used for the generation of the standard curves. Parallel quantification of each chemokine and the HPRT was performed for each sample using LightCycler technology (Roche Diagnostics). Briefly, tissue samples (1 mm^3) were dissociated and mRNA was extracted using an RNeasy kit (QIAGEN). After a reverse transcription step, cDNAs were PCR amplified in a final volume of 100 μL (10 minutes initial denaturation at 95°C, then 22 cycles of 30 seconds at 95°C, 30 seconds at 60°C, and 2 minutes at 72°C using outer 3′/5′ primer pairs). Each chemokine was coamplified together with HPRT sequences for each sample. Chemokines and HPRT were then quantified on each of these PCR products in LightCycler experiments performed on 1/100th of the initial PCR products. PCR conditions were the following: 1 minute initial denaturation at 95°C, followed by 40 cycles of 1 second at 95°C, 10 seconds at 60°C, and 15 seconds at 72°C with inner primers; fluorescence measurements were performed at the end of elongation steps. Chemokines and HPRT quantifications were performed in independent experiments using the same first-round serial dilution standard curve. The chemokine and HPRT were quantified in triplicate for all samples studied. Chemokine mRNA concentration was normalized to HPRT mRNA in each sample. Because baseline chemokine expression levels might be different between animals, the results are presented as a fold expression over a reference organ chosen to present low and stable expression for the given chemokine in the 4 animals

(ie, jejunum for CCL19, skin for CCL20, and lung for both CCL21 and CCL25).[27]

Plasma cytokine quantification

Cytokines in the plasma were quantified using the human 27-Plex and 23-Plex kits (Bio-Rad) following the manufacturer's instructions. Quantifications were performed in quadruplicate on 50 μL plasma. Of the 50 molecules detected by these kits, 25 cross-reacted with their simian orthologs (IL-1β, IL-1RA, IL-5, IL-10, IL-12, IL-13, IL-16, MCP-1, Eotaxin, granulocyte colony-stimulating factor, interferon-α [IFN-α], IFN-γ, CCL3, CCL4, CCL-5, CCL-7, CCL-27, CXCL8, CXCL9, migration inhibitory factor-3 [MIF-3], nerve growth factor-β, stromal-derived factor-1, stem cell factor, tumor necrosis factor-related apoptosis-inducing ligand, and stem cell growth factor-β). Baseline values for these molecules in rhesus macaques were on the same order of magnitude as their human counterparts. Results obtained on a BioPlex instrument were analyzed with BioPlex software.

Statistical analysis

Statistical analyses (Mann-Whitney and paired Student *t* tests) were performed using the VassarStats website (http://faculty.vassar.edu/lowry/VassarStats.html) and the StatView F-4.5 statistical software package (Abacus Concepts).

Results

Injection of R-sIL-7gly leads to an immediate drop in all peripheral T-cell subsets

Five healthy rhesus macaques (no. 14424, no. 14694, no. 26007-2, no. 41127-2, and no. 40885-2) were subcutaneously inoculated with 80 μg/kg of body weight of R-sIL-7gly, as described in "Animal care and treatment." As observed in IL-7–treated patients, all R-sIL-7gly–treated animals demonstrated a strong peripheral lymphopenia during the first day after injection (Figure 1A).[25,28] Notably, although T-cell increase was not observed at day 7 in macaque no. 40885 (designated a poor responder), the initial decrease in lymphocyte counts was also observed in this animal. In contrast, noninjected control animals (no. 21045 and no. 26007) sampled on the same schedule as the treated monkeys did not show a significant change in their circulating lymphocyte counts (Figure 1A right panel, open symbols). More importantly, in an animal extensively immunized against nonglycosylated recombinant simian IL-7 (no. 17021) and presenting high titers of anti–R-sIL-7–neutralizing antibodies (> 1/2500), injection of R-sIL-7gly did not lead to any substantial change in lymphocyte counts (Figure 1A right panel, black diamonds). Four months later, when all the measured parameters had returned to baseline levels, a second injection of R-sIL-7gly given to no. 14424 and no. 14694 led to a similar drop in circulating lymphocytes (see supplemental Figure 1, available on the *Blood* website; see the Supplemental Materials link at the top of the online article).

Most of the observed lymphocyte decline occurred in T-cell subsets. Indeed, up to 85% of the $CD4^+$ and $CD8^+$ T cells had disappeared from circulating blood by 6 hours after R-sIL-7gly injection ($P < .01$ or $P < .05$ in both $CD4^+$ and $CD8^+$ at H6, H12, H24, and H48; Figure 1B-C). In contrast, untreated control monkeys and the immunized animal demonstrated less than a 20% decline in circulating $CD4^+$ and $CD8^+$ T-cell counts (Figure 1B-C right panels, open symbols and black diamonds), ruling out a consequence resulting from repeated blood sampling. This demonstrates that T-cell depletion was a direct consequence of the R-sIL-7gly injection. In all treated monkeys, B-cell counts were much less affected by the R-sIL-7gly treatment (Figure 1D).

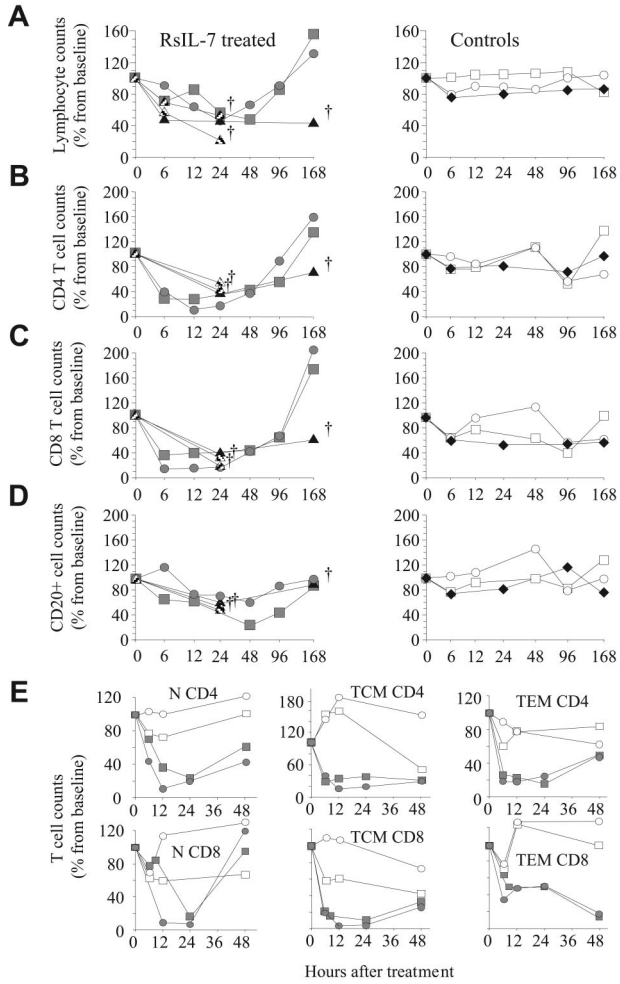

Figure 1. Injection of R-sIL-7gly rapidly induces major circulating T-cell loss in healthy rhesus macaques. Total lymphocyte (A), $CD4^+$ T-cell (B), $CD8^+$ T-cell (C), and $CD20^+$ B-cell counts (D) were measured over 1 to 7 days in 5 R-sIL-7gly–injected healthy rhesus macaques (no. 14424, ■; no. 14694, ●; no. 26007-2 and no. 41127-2, ◬; no. 40885-2, ▲; left panels), in 2 untreated control animals (no. 21045 and no. 26007, ○ and □; right panels), and in an animal previously immunized against simian IL-7 and presenting high levels of neutralizing antibodies that also received R-sIL-7 at day 0 (no. 17021, ◆; right panels). Three monkeys were killed at day 1 (no. 26007-2 and no. 41127-2) or at day 7 (no. 40885-2). Compared with baseline, lymphocyte counts drop reached statistical significance at H24 ($P < .05$), whereas both $CD4^+$ and $CD8^+$ counts were significantly reduced at H6, H12 ($P < .01$), H24, and H48 ($P < .05$). (E) Evolution of naive, central memory, and effector memory $CD4^+$ and $CD8^+$ T-cell counts in R-sIL-7gly–injected rhesus macaques (no. 14424 and no. 14694, ■and ●) and untreated controls (no. 21045 and no. 26007, ○ and □).

We next analyzed the evolution of naive, central memory, and effector memory T cells as defined by CD95 and CD28 expression in $CD4^+$ and $CD8^+$ T cells.[29] In rhesus macaques, all T-cell subsets express the IL-7 receptor α chain (CD127), probably explaining their sensitivity to IL-7. The $CD4^+$ and $CD8^+$ T-cell drop that occurs during the first day after R-sIL-7 injection is a consequence of naive ($CD95^-CD28^+$), central memory T cell (TCM; $CD95^+CD28^+$), and effector memory T cell (TEM; $CD95^+CD28^-$) T-cell depletion (Figure 1E).

Two nonexclusive hypotheses could explain such a drastic and sudden drop in circulating T-cell counts: (1) either lymphopenia

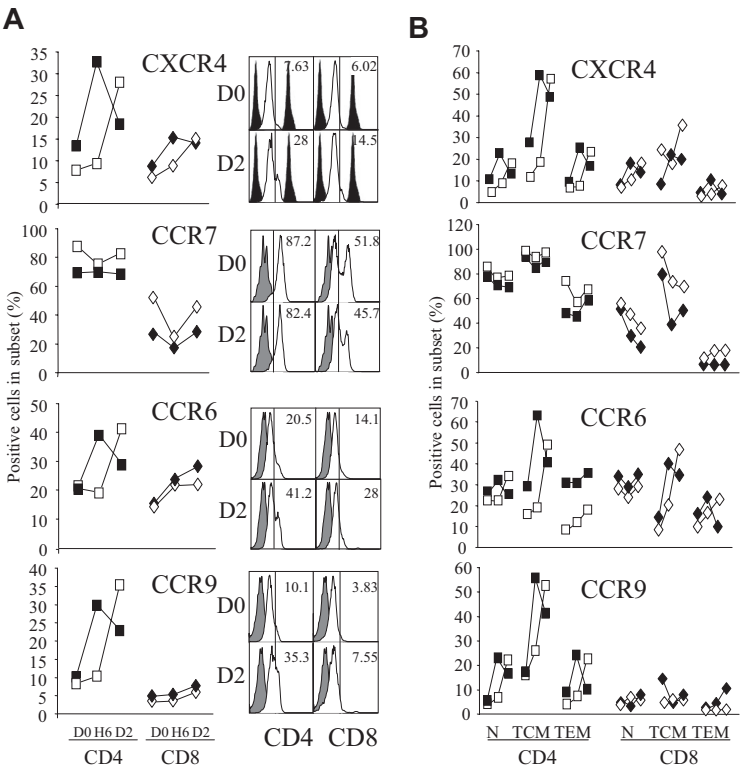

Figure 2. Evolution of chemokine receptor expression in R-sIL-7–treated macaques. (A) CXCR4, CCR7, CCR6, and CCR9 expression was FACS-quantified on circulating $CD4^+$ and $CD8^+$ T cells at H0, H6, and day 2 after R-sIL-7gly injection in healthy rhesus macaques (no. 14424, white symbols; no. 14694, black symbols). Representative FACS is shown for CD4 T cells (left histograms) and CD8 T cells (right histograms). Gray histograms represent chemokine receptor-negative cells. Percentages of chemokine receptor-positive cells are shown for each sample. (B) The evolution of CXCR4, CCR6, CCR7, and CCR9 expression on naive, TCM, and TEM $CD4^+$ (left panels on each graph) and $CD8^+$ (right panels) was measured by FACS analysis in R-sIL-7gly–injected healthy rhesus macaques (no. 14424, white symbols; no. 14694, black symbols). For each T-cell subset, chemokine expression was measured at H0, H6, and D2 (left to right).

was a consequence of massive cell death induced by pharmacologic plasma cytokine concentration and/or (2) the injection of R-sIL-7gly induced T-cell migration out of the blood.

R-sIL-7gly injection does not induce T-cell apoptosis

We first explored T-cell apoptosis in the blood (sampled at H0, H6, and day 4 after R-sIL-7gly injection) of macaques no. 14424 and no. 14694. The active form of caspase 3, caspase 8, or caspase 9 (supplemental Figure 2A) remained barely detectable in the tested samples, demonstrating that programmed cell death cannot account for the observed massive depletion of circulating T cells. Moreover, the distribution of $CD4^+$ and $CD8^+$ T cells in the axillary lymph nodes remained unchanged throughout the first days after R-sIL-7gly injection, whereas CD127 expression was strongly down-modulated (supplemental Figure 2B). Again, caspase 3, caspase 8, and caspase 9 activation as well as DNA fragmentation remained negative in these organs (supplemental Figure 2C-D). This again shows that, despite good tissue distribution in the lymph nodes, R-sIL-7gly did not induce massive T-cell apoptosis in the secondary lymphoid organs.

The absence of apoptosis in both lymph nodes and peripheral blood suggests that R-sIL-7gly–induced peripheral lymphopenia might be a consequence of T-cell redistribution from blood to organs. Because many lymphoid and nonlymphoid organs represent the usual homing sites for T lymphocytes, we further investigated the expression of molecules potentially involved in T-cell migration.

In vivo R-sIL-7gly–stimulated circulating T cells overexpress chemokine receptors

We investigated the expression of chemokine receptors implicated in T-cell homing into secondary lymphoid organs (CCR7 and CXCR4), the colon (CCR6), and the small bowel (CCR9), the principal homing organs targeted by T lymphocytes. As observed after in vitro IL-7 stimulation,[14] a strong increase of CXCR4 expression was observed in the $CD4^+$ and, to a lesser extent, the $CD8^+$ subsets (Figure 2A top panel).

In contrast, we did not observe significant modification of the expression level of CCR7 in the treated monkeys. However, in healthy rhesus macaques, the majority of circulating T cells expressed significant levels of CCR7 (70%-90% in $CD4^+$ T cells and 25%-50% in $CD8^+$ T cells; Figure 2A second panel), suggesting that CCR7-mediated T-cell homing is indeed possible and depends only on the expression of CCR7 ligands (CCL19 and CCL21).

Finally, by 48 hours after R-sIL-7gly treatment, a 1.5- to 2-fold increase of CCR6-expressing cell frequency was observed in both $CD4^+$ and $CD8^+$ subsets. In contrast, CCR9 expressing cell frequency was only increased in $CD4^+$ T cells (23%-35% at day 2 compared with 8%-10% at baseline) while remaining unchanged in $CD8^+$ T cells. Both CCR6 and CCR9 overexpression was maintained for at least 4 days (Figure 2A bottom panels).

CCR6, CCR7, CCR9, and CXCR4 expression remained stable over time in both the noninjected monkeys and the immunized animal that received R-sIL-7gly injection (data not shown).

These data demonstrate that R-sIL-7gly injection immediately triggers chemokine receptor expression by circulating T cells, allowing T-cell redistribution.

The analysis of chemokine receptor expression in the various T-cell subsets showed that these cells respond differently to R-sIL-7gly stimulation by expressing a particular set of chemokine receptors (Figure 2B). $CD4^+$ TCM demonstrated a major increase of CCR6, CCR9, and/or CXCR4 expression, whereas CCR7 expression remained high in this subset (Figure 2B). Similarly CXCR4, CCR6, and CCR9 were overexpressed by naive and TEM $CD4^+$ T cells (Figure 2B). In the $CD8^+$ subsets, R-sIL-7gly treatment induces the overexpression of both CXCR4 and CCR6 in

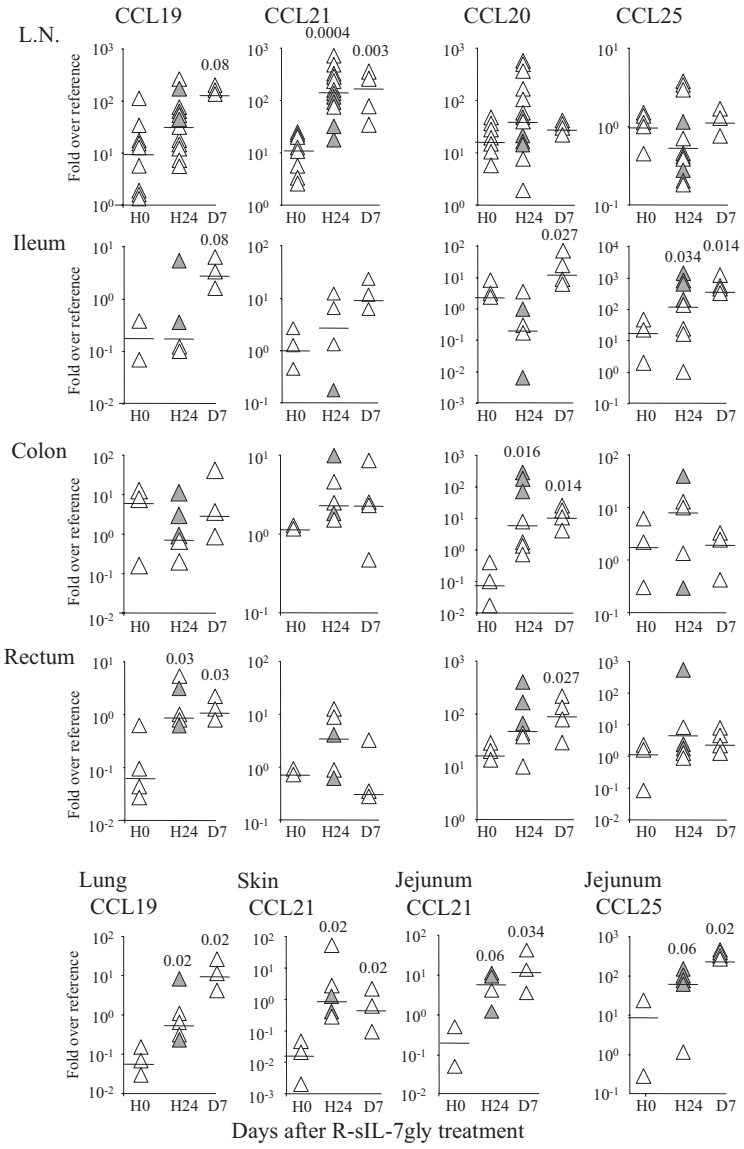

Figure 3. R-sIL-7gly injection induces chemokine production in organs. CCL19, CCL20, CCL21, and CCL25 mRNAs were quantified in lymph nodes, jejunum, ileum, colon, rectum, lung, and skin from healthy rhesus macaques killed at H0, H24, and D7 after R-sIL-7gly injection. Each symbol represents an individual quantification; gray and white symbols at H24 represent 2 individual macaques. Chemokine mRNA quantifications were normalized to HPRT mRNA in each sample and are presented as fold expression over a reference organ in which the expression of the given chemokine was low and stable over the experiment (ie, jejunum for CCL19, skin for CCL20, and lung for both CCL21 and CCL25). Statistical analyses (Mann-Whitney test) between H0 and either H24 or D7 are shown on top. Horizontal bars represent medians.

TCM and only CXCR4 in naive T cells. In these 2 subsets, CCR7 expression was reduced on treatment (Figure 2B). Finally, the expression of the 4 receptors in the TEM $CD8^+$ subset remained low (Figure 2B).

Chemokines implicated in T-cell homing are locally produced in organs

To precisely analyze the different organs that may receive the migrating T cells, macaques no. 26007-2 and no. 41127-2 were killed 24 hours after IL-7 treatment (ie, at the peak of T-cell depletion) and animal no. 40885-2 at day 7 after injection. At autopsy, axillary, inguinal, and mesenteric lymph nodes, ileum, jejunum, colon, rectum, as well as skin and lungs were sampled. Similar samples were taken from an animal killed without R-sIL-7gly injection (no. 21045-2). Messenger RNAs coding for CCL19 (CCR7 ligand), CCL20 (CCR6 ligand), CCL21 (CCR7 ligand), and CCL25 (CCR9 ligand) were quantified in several small pieces ($\pm$ 1 mm^3) from all tissue samples (Figure 3).

CCL21 mRNA levels were increased in the lymph nodes of macaques killed at day 1 and at day 7 (13- and 14-fold over baseline values, respectively, $P = .001$ and $P = .003$, Figure 3). CCL19 expression was also elevated in the lymph nodes at day 7 (12-fold increase over baseline, $P = .08$). Of note, similar chemokine expression was observed in inguinal, axillary, and mesenteric lymph nodes. Moreover, CCL19 was preferentially overexpressed in the rectum (14- and 19-fold over baseline at day 1 and day 7, $P = .03$, Figure 3) and in the lungs (9- and 157-fold increase, $P = .02$; Figure 3 bottom panels), whereas CCL21 was found overexpressed in the skin (59- and 28-fold over baseline at day 1 and day 7, respectively, $P = .02$; Figure 3 bottom panels) and in the jejunum (58- and 28-fold, $P = .06$ and $P = .034$; Figure 3 bottom panels). In contrast, these chemokines remained at baseline levels in the other tested organs.

Similarly, CCL25 mRNA concentration was increased in the ileum and jejunum (9- and 29-fold at day 1 and day 7 in the ileum, $P = .034$ and $P = .014$; 7- and 54-fold in the jejunum, $P = .06$ and $P = .02$; Figure 3).

Finally, CCL20 mRNA concentration rose in the colon and rectum (83- and 151-fold at day 1 and day 7 in the colon, $P = .016$ and $P = .014$; 3- and 5-fold in the rectum, $P = .027$ at day 7; Figure 3).

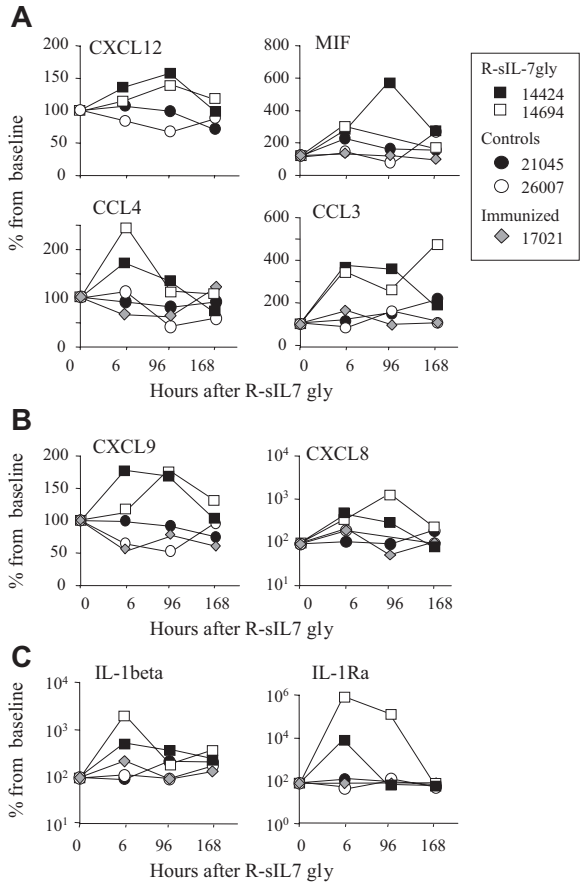

Figure 4. Quantification of plasma cytokines after R-sIL-7gly injection. Plasma concentration of various cytokines (IL-1β, IL-1RA, IL-5, IL-10, IL-12, IL-13, IL-16, MCP-1, Eotaxin, granulocyte colony-stimulating factor, IFN-α, IFN-γ, CCL3, CCL4, CCL5, CCL-7, CCL27, CXCL8, CXCL9, MIF-3, nerve growth factor-β, stromal-derived factor-1, stem cell factor, tumor necrosis factor-related apoptosis-inducing ligand, and stem cell growth factor-β) was quantified over a week in animals receiving a single dose of R-sIL-7gly injection (no. 14424 and no. 14694, ■ and □, respectively) and in control animals using BioPlex assays. Control animals were no. 21045 and no 26007 not receiving IL-7gly (● and ○, respectively) and no. 17021 immunized against R-sIL-7 before R-sIL-7gly treatment (◇). This animal presented high levels of anti–IL-7–neutralizing antibodies. Only cytokines demonstrating significant variation are shown. (A) Cytokines implicated in LN homing. (B) Cytokines implicated in migration into nonlymphoid organs. (C) Molecules playing a role in transendothelial migration.

These data demonstrate that the classic T-cell homing sites were responding to R-sIL-7gly injection by the induction of organ-specific chemokine mRNA production, again suggesting T-cell homing into these different organs.

R-sIL-7gly injection leads to the expression of various molecules implicated in T-cell trafficking

Using the human Bio-Plex assay, we next evaluated the evolution of plasma concentration of various molecules implicated in T-cell trafficking and inflammation. Of the 50 molecules screened by the 27-Plex and 23-Plex kits, 25 cross-reacted with their simian orthologs (see "Plasma cytokine quantification"). A transient rise of plasma concentration of CXCL12 (1.5-fold increase at H96), MIF (3- to 6-fold), CCL3 (3- to 4-fold increase at H6), and CCL4 (1.5- to 2-fold), molecules known to participate in T-cell homing into lymphoid organs,[30,31] was observed in both treated macaques (Figure 4A). Similarly, some molecules implicated in T-cell homing into nonlymphoid organs were also overexpressed after IL-7 treatment: CXCL9 (1.5- to 2-fold) and CXCL8 (5- to 10-fold)[32,33] (Figure 4B). Finally, plasma concentrations of IL-1beta and IL-1RA, molecules implicated in transendothelial migration,[34] were augmented after R-sIL-7gly injection (10- to 20-fold and 10- to 100-fold, respectively; Figure 4C).

These data demonstrate that, in addition to chemokine and chemokine receptor expression, R-sIL-7gly injection leads to significant and reproducible in vivo production of various molecules involved in T-cell trafficking.

Circulating T cells home to various peripheral organs

To confirm that R-sIL-7gly injection effectively triggers T-cell homing to the lymph nodes, gut, and skin, tissue samples from animals no. 26007-2, no. 41127-2 (killed 24 hours after R-sIL-7gly injection), no. 40885-2 (killed at day 7), and no. 21045-2 (noninjected animal) were subjected to immunohistologic labeling with anti-CD3 monoclonal antibodies (Figure 5). T-cell infiltration was observed in the skin and the lamina propria of the ileum, the colon, and the rectum (Figure 5A-F). Quantifying $CD3^+$ T cells in 7 to 10 fields (0.09 mm^2 each) randomly selected from 4 slides for each organ confirmed that the number of $CD3^+$ T cells per field was significantly increased by day 1 in the skin ($P = .001$; Figure 5A right panel), the ileum ($P = .003$; Figure 5D right panel), the colon ($P = .018$; Figure 5E right panel), and the rectum ($P = .05$; Figure 5F right panel). In all organs but the colon, T-cell numbers remained significantly higher at day 7 compared with the control animal. In contrast, the density of $CD3^+$ T cells was not significantly modified in the lymph nodes. Details of the immunochemistry experiments are described in "Immunohistochemistry."

These data confirmed that R-sIL-7gly induces T-cell homing into various nonlymphoid organs, including the lamina propria of several parts of the gut (ileum, colon, and rectum) and skin. Moreover, the expression of CCR7 and CXCR4 on circulating T cells (Figure 2), the increase of CXCL12 plasma concentration (Figure 4), and the production of CCL19 and/or CCL21 mRNA in lymph nodes (Figure 3) also suggest homing into secondary lymphoid organs. Similarly, the production of CCL19 in the ileum and the rectum and that of CCL21 in the jejunum (Figure 3) suggest that R-sIL-7gly injection also triggers T-cell migration into the lymphoid follicles of the gut.

T cells start cycling in the organs before migrating back into peripheral blood

After the initial decrease in circulating T-cell numbers, we observed a rebound in T-cell counts starting at day 4. In all T-cell subsets, the gain represents 50% to 150% of the initial circulating T-cell counts at day 7 (Figure 1 and supplemental Figure 1). At that time, repopulating T cells were indeed cycling as demonstrated by the frequency of Ki-67^+ T cells (20%–30% and up to 60% at day 7 in the $CD4^+$ and $CD8^+$ T-cell subset, respectively; Figure 6A). In contrast, during the first 2 days after R-sIL-7gly injection, when circulating T cells were overexpressing chemokine receptors as well as the antiapoptotic molecule Bcl-2 (Figure 6B), T-cell cycling was not yet evidenced in circulating blood. Interestingly, in the lymphoid tissue (lymph node and intestinal follicles) in the lamina propria of the ileum, the colon, and the rectum as well as in the skin, a statistically significant increase of Ki-67 expression was observed as early as 1 day after R-sIL-7gly injection ($P < .05$; Figure 6C-D). Details of the immunochemistry experiments are described in "Immunohistochemistry."

This demonstrates that T-cell cycling is initiated as early as 1 day after IL-7 stimulation within the organs where the injected

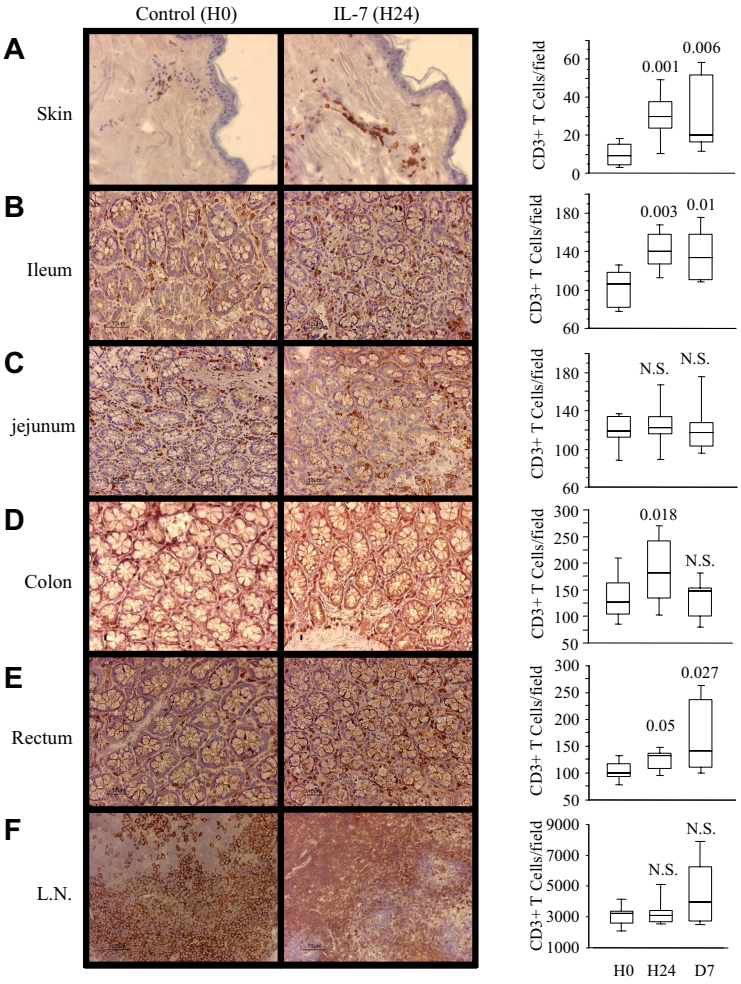

Figure 5. R-sIL-7gly injection induces T-cell homing into organs. Rhesus macaques injected with R-sIL-7gly (80 μg/kg) were killed at D1 (left pictures) and compared with untreated animals (right pictures). $CD3^+$ cells were identified by immunohistochemistry in skin (A), jejunum (B), ileum (C), colon (D), rectum (E), and lymph node (F) samples. Magnification: ×100. $CD3^+$ T-cell quantifications, performed on 7 to 10 fields (0.09 mm^2) randomly selected from 4 slides for each organ in macaques killed at H0, H24, and D7 after R-sIL-7gly injection, are shown on the right. Statistical differences between H0 and either H24 or D7 are shown on top (Mann-Whitney test).

cytokine induced their migration. In contrast, the cells remaining in the blood during the first days of IL-7 stimulation were not proliferating. Cycling T cells eventually returned to the blood by day 4, leading to increased numbers of circulating T cells in the treated monkeys.

Discussion

In the last few years, therapeutic stimulation of the immune system has begun to have an increasingly important impact on medical practice. In particular, IL-2 and IL-7 are currently under clinical investigation for treatment of severe lymphopenia and have produced promising results.[7,8] The significant increase of circulating T cells observed in most IL-2–treated HIV-1–infected patients is the net result of the increase of both proliferation and apoptosis.[8] Consequently, such a treatment, even at its best, does not restore, and indeed probably reduces, T-cell repertoire diversity. Similarly, in the first patients treated with IL-7, the observed initial T-cell depletion could influence the efficacy of this treatment in restoring T-cell repertoire diversity.[7] However, we have herein demonstrated that the initial T-cell depletion observed during R-sIL-7gly treatment is not the result of massive T-cell apoptosis but is instead a consequence of massive cell redistribution.

The rapid T-cell redistribution observed in IL-7–treated macaques suggests that IL-7 concentration in the target organs is important for T-cell function. Indeed, higher IL-7 concentration is necessary to trigger in vitro T-cell cycling than to stimulate cell survival.[14] In vivo, higher local concentration might be achieved in organs where the cytokine is trapped on heparan sulfates at the stromal cell surface. Indeed, in preliminary experiments, the injection of radiolabeled IL-7 in cynomolgus macaques led to a higher concentration in lymph nodes and spleen (20.8-32.8 ng/g tissue), in the intestine (16.5, 19.1, and 21.2 ng/g in the bowel, colon, and rectum, respectively), and in the lungs (18.7 ng/g) than in the blood (3.9 ng/g). Differential expression of chemokine receptors by these different T-cell subsets (Figure 2) as well as the chemokine production in nonlymphoid tissues, such as the skin, lungs, and intestine (Figure 3), suggest a particular function for T-cell homing in these tissues. Indeed, IL-7 participates in T-cell responses to antigenic stimulation.[35-37] Moreover, most of the molecules that were induced after IL-7 treatment were described as participating in T-cell homing into these organs during inflammatory reactions.[38-42] The expression patterns of chemokines/chemokine receptors suggest that naive and memory $CD4^+$ T cells are directed to the gut through CCR6/CCL20 and/or CCR9/CCL25 expression, whereas all T-cell subsets (but the TEM $CD8^+$, which barely express CCR7) might migrate into the skin and the lungs where CCR7-ligands (CCL19, CCL21) expression is increased. The involvement of IL-7–driven T-cell homing into nonlymphoid tissues in innate and adaptive immunity remains to be clarified, but it is possible that the injection of R-sIL-7gly mimicked certain aspects of antigen-induced immune activa-

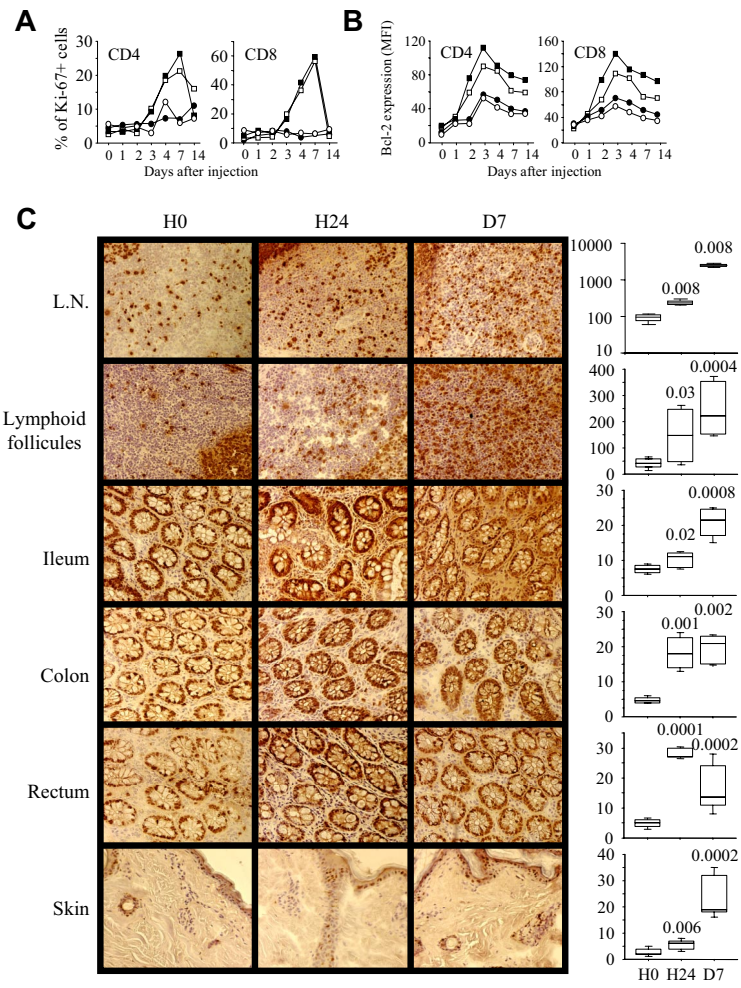

Figure 6. IL-7-induced Ki-67 and Bcl-2 expression in circulating blood and homing target organs. Initiation of cell cycling, as evidenced by the expression of Ki-67 (A) and cell survival capacity, as evidenced by Bcl-2 expression (B), were quantified in circulating $CD4^+$ and $CD8^+$ T lymphocytes in R-sIL-7gly–injected rhesus macaques (no. 14424 and no. 14694, ■ and □) compared with noninjected control animals (no. 21045 and no. 26007, ● and ○) over a 14-day period after R-sIL-7gly injection. (C) Ki-67$^+$ cells were identified in lymph nodes, in Peyer patches (ileum), in the lamina propria (ileum, colon, and rectum) and in the skin of animals killed at H0, H24, and D7 after R-sIL-7gly injection. Magnification: ×100. Ki-67$^+$ T-cell quantifications, performed on 5 to 6 fields (0.09 mm^2) randomly selected from 4 slides for each organ in macaques killed at H0, H24, and D7 after R-sIL-7gly injection are shown on the right. Statistical differences between H0 and either H24 or D7 are shown on top (Mann-Whitney test).

tion by initiating T-cell migration to the sites of frequent pathogen intrusion.

Both in vitro and in vivo, IL-7 induces CXCR4 up regulation by T lymphocytes, suggesting a role of IL-7 in T-cell homing into CXCL12-rich tissues. Indeed, our in vivo experiments showed that IL-7–induced CXCR4 overexpression coincides with an increased CXCL12 plasma concentration (Figures 2,4). In addition, we showed that R-sIL-7gly injection stimulates CCL19 and CCL21 production by secondary lymphoid organs in which all T-cell subsets could thus be recruited through constitutive CCR7 expression (Figures 2-3). Although homing into lymph nodes is difficult to demonstrate in the macaque model, these data confirm observations made in mice, demonstrating the importance of lymph nodes in the regulation of naive T-cell homeostasis through IL-7 and CCL19 production,[6] but also through CXCR4/CXCL12 expression. Finally, the fact that at day 1 after R-sIL-7gly injection, T-cell cycling occurs in the lymph nodes and intestinal follicles whereas it remains undetectable in blood further reinforces this conclusion and suggests that homing to these organs is crucial for complete in vivo IL-7 stimulation (Figure 6C).

The local chemokine production in the different target organs suggests that resident cells are responsive to IL-7. Interestingly, monocytes and dendritic cells were shown to be essential for IL-7–induced proliferation[43,44] and, together with fibroblasts, to produce most of the proteins observed in R-sIL-7gly–treated macaques.[44-47] Further investigation of the impact of IL-7 on the production of these molecules by cells located in tissues will help in understanding both homeostatic and inflammatory homing processes induced by IL-7.

In conclusion, we have identified a novel property of IL-7 that, when injected to healthy rhesus macaques, rapidly initiates massive T-cell homing into secondary lymphoid organs and various epithelia. This effect is a direct consequence of both an increased expression of chemokine receptors (CXCR4, CCR6, and CCR9) by circulating T cells and the initiation of chemokine transcription in the target organs. Homing processes were facilitated by the IL-7–dependent production of various molecules implicated in transendothelial cell migrations (IL-1β, IL-1RA, CCL3, and CCL4). However, other chemokine/chemokine receptors as well as other molecules implicated in T-cell trafficking can also be involved in the IL-7–induced cell migrations, in particular in the $CD8^+$ subsets. By targeting circulating T cells at the natural sites of IL-7 production, subsequently leading to T-cell proliferation, IL-7–induced T-cell homing appears to play an important role in the homeostatic regulation of peripheral T-cell pools. As previously observed, T-cell proliferation eventually leads to a 1.5- to 2.5-fold increase in circulating T cells a week after IL-7 treatment.[25,28] Interestingly, the IL-7-induced homing process drove circulating T cells to different organs, including several parts of the gut where massive T-cell proliferation subsequently occurs. Considering the results presented here and their possible impact on the treatment of HIV-1–infected patients, it would appear to be of great importance to evaluate the potential of IL-7, in combination with highly active antiretroviral therapy in stimulating the T-cell repopulation of the gut, known to be massively T-cell depleted early in the

course of HIV infection[48] and thereby opening the patient to the effects of opportunistic infections and malignancies, which are frequently associated with a weakened immune system in this patient population.[48]

Acknowledgments

The authors thank Dr Cécile Butor for samples from healthy macaque, Drs Rafick-Pierre Sékaly, Jean-François Bureau, Fernando Arenzana-Seisdedos, Antonio Freitas, and Ali Amara for helpful discussion and a critical reading of the manuscript, and Richard Keatinge for his valuable help in preparing the manuscript.

This work was supported by Institut Pasteur, Cytheris SA, and the Agence Nationale de Recherches sur le SIDA et les hepatites virales (ANRS). This work was carried out in partial fulfillment of the doctoral thesis of R.P. at the Université Paris 6 and the doctoral thesis of D.G. at the Université Paris 7, France. D.G. was the recipient of a PhD ANRS scholarship. S.B. was successively the recipient of a SIDACTION postdoctoral grant and an ANRS postdoctoral grant. V.M. was the recipient of an ANRS postdoctoral grant.

Authorship

Contribution: S.B. performed research, analyzed data, and wrote the manuscript; S.R., D.G., R.P., V.M., and C.S. performed research; B.A. and I.R. contributed vital new reagents; P.L. participated with animal care; M.M. designed research and contributed vital new reagents; and R.C. designed research, analyzed data, and wrote the manuscript.

Conflict-of-interest disclosure: M.M. is the CEO and Founder of Cytheris. B.A. and I.R. are employees of Cytheris. S.B. is presently an employee of Cytheris. Cytheris develops recombinant interleukin-7 as a global immune enhancer and partly supported this work. The remaining authors declare no competing financial interests.

Correspondence: Rémi Cheynier, Département de Virologie, Institut Pasteur, 25-28, Rue du Docteur Roux 75724 Paris Cedex 15, France; e-mail: remi.cheynier@pasteur.fr.

References

1. Milne CD, Fleming HE, Zhang Y, Paige CJ. Mechanisms of selection mediated by interleukin-7, the preBCR, and hemokinin-1 during B-cell development. *Immunol Rev.* 2004;197:75-88.
2. Guillemard E, Nugeyre MT, Chene L, et al. Interleukin-7 and infection itself by human immunodeficiency virus 1 favor virus persistence in mature CD4(+)CD8(-)CD3(+) thymocytes through sustained induction of Bcl-2. *Blood.* 2001;98:2166-2174.
3. Napolitano LA, Stoddart CA, Hanley MB, Wieder E, McCune JM. Effects of IL-7 on early human thymocyte progenitor cells in vitro and in SCID-hu Thy/Liv mice. *J Immunol.* 2003;171:645-654.
4. Fry TJ, Connick E, Falloon J, et al. A potential role for interleukin-7 in T-cell homeostasis. *Blood.* 2001;97:2983-2990.
5. Rathmell JC, Farkash EA, Gao W, Thompson CB. IL-7 enhances the survival and maintains the size of naive T cells. *J Immunol.* 2001;167:6869-6876.
6. Link A, Vogt TK, Favre S, et al. Fibroblastic reticular cells in lymph nodes regulate the homeostasis of naive T cells. *Nat Immunol.* 2007;8:1255-1265.
7. Sportes C, Hakim FT, Memon SA, et al. Administration of rhIL-7 in humans increases in vivo TCR repertoire diversity by preferential expansion of naive T-cell subsets. *J Exp Med.* 2008;205:1701-1714.
8. Sereti I, Herpin B, Metcalf JA, et al. CD4 T-cell expansions are associated with increased apoptosis rates of T lymphocytes during IL-2 cycles in HIV infected patients. *AIDS.* 2001;15:1765-1775.
9. Yoshie O, Imai T, Nomiyama H. Chemokines in immunity. *Adv Immunol.* 2001;78:57-110.
10. Ebert LM, Schaerli P, Moser B. Chemokine-mediated control of T-cell traffic in lymphoid and peripheral tissues. *Mol Immunol.* 2005;42:799-809.
11. Schaerli P, Willimann K, Lang AB, Lipp M, Loetscher P, Moser B. CXC chemokine receptor 5 expression defines follicular homing T cells with B cell helper function. *J Exp Med.* 2000;192:1553-1562.
12. Kunkel EJ, Campbell DJ, Butcher EC. Chemokines in lymphocyte trafficking and intestinal immunity. *Microcirculation.* 2003;10:313-323.
13. Johansson-Lindbom B, Agace WW. Generation of gut-homing T cells and their localization to the small intestinal mucosa. *Immunol Rev.* 2007;215:226-242.
14. Swainson L, Kinet S, Mongellaz C, Sourisseau M, Henriques T, Taylor N. IL-7-induced proliferation of recent thymic emigrants requires activation of the PI3K pathway. *Blood.* 2007;109:1034-1042.
15. Gutierrez-Ramos JC, Olsson C, Palacios R. Interleukin (IL1 to IL7) gene expression in fetal liver and bone marrow stromal clones: cytokine-mediated positive and negative regulation. *Exp Hematol.* 1992;20:986-990.
16. Oosterwegel MA, Haks MC, Jeffry U, Murray R, Kruisbeek AM. Induction of TCR gene rearrangements in uncommitted stem cells by a subset of IL-7 producing, MHC class-II-expressing thymic stromal cells. *Immunity.* 1997;6:351-360.
17. Galy AH, de Waal Malefyt R, Barcena A, Peterson SM, Spits H. Untransfected and SV40-transfected fetal and postnatal human thymic stromal cells: analysis of phenotype, cytokine gene expression and cytokine production. *Thymus.* 1993;22:13-33.
18. Watanabe M, Ueno Y, Yajima T, et al. Interleukin 7 is produced by human intestinal epithelial cells and regulates the proliferation of intestinal mucosal lymphocytes. *J Clin Invest.* 1995;95:2945-2953.
19. de Saint-Vis B, Fugier-Vivier I, Massacrier C, et al. The cytokine profile expressed by human dendritic cells is dependent on cell subtype and mode of activation. *J Immunol.* 1998;160:1666-1676.
20. Heufler C, Topar G, Grasseger A, et al. Interleukin 7 is produced by murine and human keratinocytes. *J Exp Med.* 1993;178:1109-1114.
21. Madrigal-Estebas L, McManus R, Byrne B, et al. Human small intestinal epithelial cells secrete interleukin-7 and differentially express two different interleukin-7 mRNA transcripts: implications for extrathymic T-cell differentiation. *Hum Immunol.* 1997;58:83-90.
22. Clarke D, Katoh O, Gibbs RV, Griffiths SD, Gordon MY. Interaction of interleukin 7 (IL-7) with glycosaminoglycans and its biological relevance. *Cytokine.* 1995;7:325-330.
23. Borghesi LA, Yamashita Y, Kincade PW. Heparan sulfate proteoglycans mediate interleukin-7-dependent B lymphopoiesis. *Blood.* 1999;93:140-148.
24. Banwell CM, Partington KM, Jenkinson EJ, Anderson G. Studies on the role of IL-7 presentation by mesenchymal fibroblasts during early thymocyte development. *Eur J Immunol.* 2000;30:2125-2129.
25. Beq S, Nugeyre MT, Ho Tsong Fang R, et al. IL-7 induces immunological improvement in SIV-infected rhesus macaques under antiviral therapy. *J Immunol.* 2006;176:914-922.
26. Nugeyre MT, Monceaux V, Beq S, et al. IL-7 stimulates T-cell renewal without increasing viral replication in simian immunodeficiency virus-infected macaques. *J Immunol.* 2003;171:4447-4453.
27. Clay CC, Rodrigues DS, Brignolo LL, et al. Chemokine networks and in vivo T-lymphocyte trafficking in nonhuman primates. *J Immunol Methods.* 2004;293:23-42.
28. Fry TJ, Moniuszko M, Creekmore S, et al. IL-7 therapy dramatically alters peripheral T-cell homeostasis in normal and SIV-infected nonhuman primates. *Blood.* 2003;101:2294-2299.
29. Pitcher CJ, Hagen SI, Walker JM, et al. Development and homeostasis of T-cell memory in rhesus macaque. *J Immunol.* 2002;168:29-43.
30. Schall TJ, Bacon K, Camp RD, Kaspari JW, Goeddel DV. Human macrophage inflammatory protein alpha (MIP-1 alpha) and MIP-1 beta chemokines attract distinct populations of lymphocytes. *J Exp Med.* 1993;177:1821-1826.
31. Tanaka Y, Adams DH, Hubscher S, Hirano H, Siebenlist U, Shaw S. T-cell adhesion induced by proteoglycan-immobilized cytokine MIP-1 beta. *Nature.* 1993;361:79-82.
32. Santamaria Babi LF, Moser B, Perez Soler MT, et al. The interleukin-8 receptor B and CXC chemokines can mediate transendothelial migration of human skin homing T cells. *Eur J Immunol.* 1996;26:2056-2061.
33. Gasperini S, Marchi M, Calzetti F, et al. Gene expression and production of the monokine induced by IFN-gamma (MIG), IFN-inducible T-cell alpha chemoattractant (I-TAC), and IFN-gamma-inducible protein-10 (IP-10) chemokines by human neutrophils. *J Immunol.* 1999;162:4928-4937.
34. Dinarello CA, Savage N. Interleukin-1 and its receptor. *Crit Rev Immunol.* 1989;9:1-20.
35. Peschon JJ, Morrissey PJ, Grabstein KH, et al. Early lymphocyte expansion is severely impaired in interleukin 7 receptor-deficient mice. *J Exp Med.* 1994;180:1955-1960.

36. Sin JI, Kim J, Pachuk C, Weiner DB. Interleukin 7 can enhance antigen-specific cytotoxic-T-lymphocyte and/or Th2-type immune responses in vivo. *Clin Diagn Lab Immunol.* 2000;7:751-758.

37. Shen CH, Ge Q, Talay O, Eisen HN, Garcia-Sastre A, Chen J. Loss of IL-7R and IL-15R expression is associated with disappearance of memory T cells in respiratory tract following influenza infection. *J Immunol.* 2008;180:171-178.

38. Taub DD, Conlon K, Lloyd AR, Oppenheim JJ, Kelvin DJ. Preferential migration of activated CD4+ and CD8+ T cells in response to MIP-1 alpha and MIP-1 beta. *Science.* 1993;260:355-358.

39. Agostini C, Facco M, Siviero M, et al. CXC chemokines IP-10 and mig expression and direct migration of pulmonary CD8+/CXCR3+ T cells in the lungs of patients with HIV infection and T-cell alveolitis. *Am J Respir Crit Care Med.* 2000;162:1466-1473.

40. Yamanaka K, Clark R, Rich B, et al. Skin-derived interleukin-7 contributes to the proliferation of lymphocytes in cutaneous T-cell lymphoma. *Blood.* 2006;107:2440-2445.

41. Staton PJ, Carpenter AB, Jackman SH. IL-7 is a critical factor in modulating lesion development in Skn-directed autoimmunity. *J Immunol.* 2006;176:3978-3986.

42. Bernhagen J, Krohn R, Lue H, et al. MIF is a noncognate ligand of CXC chemokine receptors in inflammatory and atherogenic cell recruitment. *Nat Med.* 2007;13:587-596.

43. McKinlay A, Radford K, Kato M, et al. Blood monocytes, myeloid dendritic cells and the cytokines interleukin (IL)-7 and IL-15 maintain human CD4+ T memory cells with mixed helper/regulatory function. *Immunology.* 2007;120:392-403.

44. Stagg AJ, Hart AL, Knight SC, Kamm MA. The dendritic cell: its role in intestinal inflammation and relationship with gut bacteria. *Gut.* 2003;52:1522-1529.

45. Sallusto F, Palermo B, Lenig D, et al. Distinct patterns and kinetics of chemokine production regulate dendritic cell function. *Eur J Immunol.* 1999;29:1617-1625.

46. Shortman K, Liu YJ. Mouse and human dendritic cell subtypes. *Nat Rev Immunol.* 2002;2:151-161.

47. Mora JR, Bono MR, Manjunath N, et al. Selective imprinting of gut-homing T cells by Peyer's patch dendritic cells. *Nature.* 2003;424:88-93.

48. Brenchley JM, Schacker TW, Ruff LE, et al. CD4+ T-cell depletion during all stages of HIV disease occurs predominantly in the gastrointestinal tract. *J Exp Med.* 2004;200:749-759.